The 9th European Congress on Computational Methods in Applied Sciences and Engineering
ECCOMAS Congress 2024
3 – 7 June 2024, Lisboa, Portugal

APPLICATION OF MECHANICAL MODELLING STRATEGIES TO THE HYGROTHERMAL ANALYSIS OF MASONRY WALLS

RAFAEL RAMIREZ[*], ALEJANDRO JIMÉNEZ-RÍOS[†], BAHMAN GHIASSI[‡] AND PAULO B. LOURENÇO[*]

[*] Department of Civil Engineering, ISISE, ARISE, University of Minho
Universidade do Minho, Campus de Azurém s/n, 4800-058 Guimarães, Portugal
rramirez@civil.uminho.pt; https://orcid.org/0000-0002-1369-6209
pbl@civil.uminho.pt; https://orcid.org/0000-0001-8459-0199

[†] Department of Architecture & Civil Engineering, University of Bath
North Road, Claverton Down, Bath BA2 7AY, United Kingdom
ajr225@bath.ac.uk; https://orcid.org/0000-0003-4470-255X

[‡] Department of Civil Engineering, School of Engineering, University of Birmingham
University of Birmingham, B15 2TT, Birmingham, United Kingdom
b.ghiassi@bham.ac.uk; https://orcid.org/0000-0003-4212-8961

Key words: Brick Masonry, Heat and Moisture Transport, Numerical Simulations, Mortar Joints, Multiphysics.

Summary. This study investigates the hygrothermal transport mechanisms in brick masonry, focusing on the applicability of different modelling approaches, namely detailed micro-modelling, continuous micro-modelling, discrete micro-modelling, and macro-modelling. The research addresses the challenge of balancing computational efficiency with accuracy in simulating heat and moisture transport within masonry structures. By examining a representative cross-section of a brick masonry wall subjected to external environmental loads, the study evaluates the effectiveness of these models in predicting hygrothermal behaviour. While thermal transport can be adequately represented by simplified models due to the relatively homogeneous distribution of thermal properties, moisture transport presents a greater complexity. In particular, the detailed micro-modelling approach highlights the limitations of simplified models in capturing localized moisture effects. A significant challenge arises in calibrating models for moisture transport parallel to the bed joints, where continuous lime mortar joints act as preferential moisture paths. This leads to discrepancies when applying calibration parameters derived from experiments on transport perpendicular to the bed joints. The findings of this study underscore the need for further research to refine calibration methods, explore different material combinations, and improve the accuracy of homogenization techniques, ultimately enhancing the reliability of hygrothermal simulations in masonry structures.

NOTATION			
A_w	Capillary absorption coefficient [kg/(m^2·s$^{0.5}$)]	t	Time [s]
a	Fitting parameter for adsorption isotherm [1/Pa]	V	Volume [m^3]
C_p	Specific heat capacity [J/(kg·K)]	w	Moisture content [kg/m^3]
D_w	Liquid water diffusivity [m^2/s]	w_{cap}	Capillary moisture content [kg/m^3]
g	Moisture flux [kg/(m·s^2)]	δ_a	Vapour permeability of still air [kg/(m s Pa)]
K_{IF}	Interface permeability [s/m]	γ	Diffusivity factor [–]
m	Fitting parameter for adsorption isotherm [–]	λ	Thermal conductivity [W/(m K)]
p_c	Capillary pressure [Pa]	μ	Vapour resistivity of material [–]
$p_{v,sat}$	Saturation vapour pressure [Pa]	φ	Relative humidity [–]
q	Heat flux [W/m^2]	ϕ_o	Open porosity [–]
R_{IF}	Interface resistance [m/s]	ψ	Fitting parameter for sorption isotherm [–]
R_v	Universal gas constant [J/(mol K)]	ρ	Density [kg/m^3]
T	Temperature [K]	ϑ	Temperature [ºC]

1 INTRODUCTION

The study of hygrothermal phenomena in building structures is a crucial component for understanding the broader field of building physics. These phenomena significantly impact various aspects of building performance, including thermal comfort, energy efficiency, and sustainability [1–3]. Moreover, the presence of moisture within masonry can profoundly influence the durability and structural integrity of the building [4,5]. Given these concerns, considerable efforts have been dedicated to developing sophisticated hygrothermal models (e.g., see [6]) capable of simulating the complex interactions between heat and moisture in porous building materials, such as masonry.

To achieve efficient simulations, however, it is often necessary to make assumptions and simplifications in an attempt to reduce the computational burden while maintaining accuracy. One of the most effective approaches in this regard is the use of homogenization techniques These techniques involve averaging the properties of heterogeneous materials to create a simplified, equivalent homogeneous material that can be analysed more easily. In the field of structural mechanics, homogenization has been extensively applied for the modelling and analysis of masonry, enabling engineers to predict the behaviour of complex structures with greater computational efficiency [7,8]. This approach has proven effective for structural analysis, and its potential applicability to hygrothermal simulations deserves exploration. By applying the principles developed in structural mechanics, it may be possible to create more efficient and accurate models for simulating heat and moisture transport in brick masonry.

In the modelling of masonry structures, various approaches have been developed to address the balance between computational efficiency and model accuracy. These approaches are categorized as detailed micro-modelling, continuous micro-modelling, simplified micro-modelling, and macro-modelling (**Figure 1**):

- Detailed micro-modelling involves a highly detail representation of masonry, where each component of the masonry, including individual bricks, mortar joints, and brick-mortar interfaces, is explicitly modelled. This approach provides the most accurate simulation of

the material behaviour, including interfacial effects, but requires significant computational resources.

- Continuous micro-modelling simplifies the system by representing brick and mortar with their original properties, while neglecting explicit interfaces. This method, which requires detailed material properties, slightly reduces complexity while still providing a high level of accuracy, especially in cases where explicit interfaces are to be avoided.
- Discrete micro-modelling further simplifies the masonry by modelling bricks as a continuum with equivalent properties, while interfaces simulate mortar joints and brick-mortar boundaries. This approach offers a balance between simplicity and accuracy, making it suitable when mortar properties are unknown, though it requires more geometric consideration due to the extended brick geometry.
- Macro-modelling approaches represent the entire masonry as a continuum with homogenized material properties. This method is less complex and computationally demanding but provides lower accuracy, particularly in capturing localized phenomena or interfacial effects.

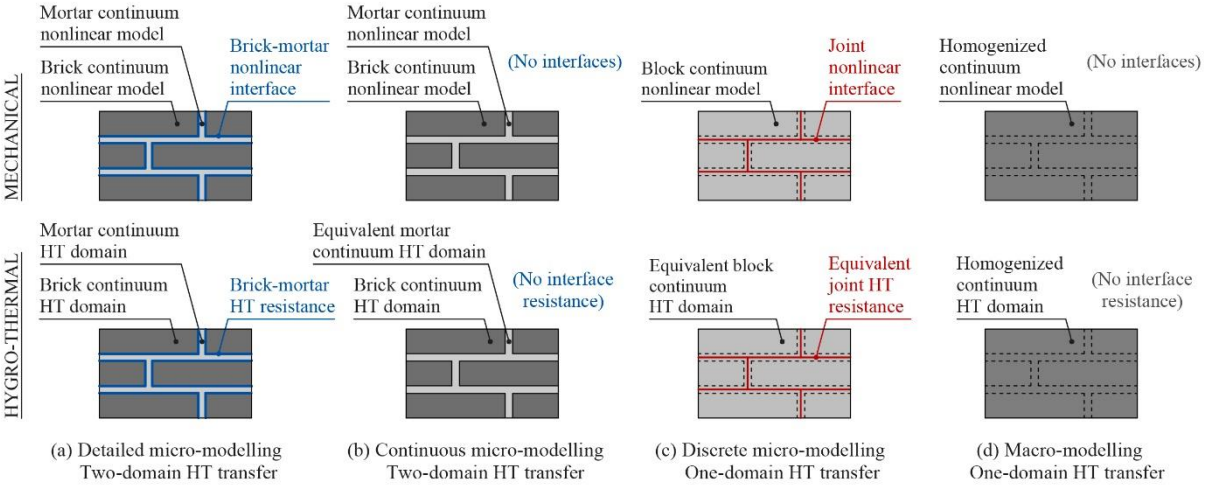

Figure 1. Modelling approaches for the simulation of masonry (adapted from [9], after [7,8]).

These approaches, while well-established in structural mechanics, have yet to be fully explored in the context of hygrothermal analysis. This study seeks to investigate the applicability of these modelling techniques to simulate the heat and moisture transport in brick masonry, evaluating their potential to provide accurate and efficient simulations in this new domain. For this purpose, the cross-section of a brick masonry wall was modelled to study moisture and heat transport under external environmental loads, such as wind-driven rain and solar radiation. The analysis considered the different modelling strategies to evaluate how each approach influences the accuracy and computational efficiency of simulating these hygrothermal phenomena.

2 METHODS

2.1 Hygrothermal problem

This section outlines the numerical model used for hygrothermal simulations and its underlying assumptions. The material is assumed as a porous medium composed of a network of interconnected pores within a solid structure. The solid phase is continuous, homogeneous, inert, isotropic, and non-deformable. The pores are assumed to be cylindrical, uniformly distributed, and isotropic throughout the material. The pore spaces are occupied by a liquid and a gaseous phase in varying proportions. The liquid phase is pure and incompressible, while the gaseous phase is modelled as an ideal mixture of dry air and water vapour at atmospheric pressure. The model does not include advective air flow, and pressure gradients are considered negligible. A local instantaneous thermodynamic equilibrium is assumed between the liquid and gaseous phases, allowing for a combined definition of global moisture content, though the contribution of water vapour to this total is negligible. The model excludes Knudsen flow, and neglects gravity effects, as capillary forces are assumed to be dominant.

The heat transport model employed in this study is defined as:

$$\rho C \frac{\partial T}{\partial t} = \nabla \cdot (\lambda \nabla T) \tag{1}$$

Additionally, the moisture transport model is described as:

$$\frac{\partial w}{\partial \varphi}\frac{\partial \varphi}{\partial t} = \nabla \cdot \left(\frac{\partial w}{\partial \varphi} D_w \nabla \varphi\right) + \nabla \cdot \left[\frac{\delta_a}{\mu} \nabla \left(\varphi\, p_{v,sat}\right)\right] \tag{2}$$

In the previous expression, D_w is an updated version of the liquid diffusivity expression defined by Künzel [10], which incorporates a diffusivity factor γ (in the original formulation $\gamma = 3.80$) to account for material characteristics and type of process (wetting/drying):

$$D_w = \gamma \cdot \left(\frac{A_w}{w_{cap}}\right)^2 \cdot 10^{3\cdot\left(\frac{w}{w_{cap}}-1\right)} \tag{3}$$

The interfaces between brick and mortar are assumed to have perfect contact for heat transport, whereas imperfect contact is assumed for moisture transport. As a result, moisture flux across the interface, g_{IF}, is modelled by introducing an interface permeability, K_{IF}, or an interface resistance R_{IF}, as follows:

$$g_{IF} = K_{IF}\frac{\partial p_c}{\partial x} = \frac{1}{\frac{1}{K_{IF}}}\frac{\partial p_c}{\partial x} = \frac{\Delta p_c}{\frac{1}{K_{IF}}\Delta x} = \frac{\Delta p_c}{R_{IF}}, \tag{4}$$

In this expression, the capillary pressure p_c is related to relative humidity through Kelvin's equation:

$$p_c = \rho_w \cdot R_v \cdot T \cdot \ln \varphi, \tag{5}$$

Therefore, assuming the validity of Kelvin's equation, the moisture flux across the interface can be expressed as:

$$g_{IF} = K_{IF}\frac{\partial p_c}{\partial \varphi}\frac{\partial \varphi}{\partial x} = K_{IF}\frac{\rho_w \cdot R_v \cdot T}{\varphi}\frac{\partial \varphi}{\partial x} = \frac{\rho_w \cdot R_v \cdot T}{\varphi}\frac{\Delta \varphi}{\frac{1}{K_{IF}}\Delta x} = \frac{\rho_w \cdot R_v \cdot T}{\varphi}\frac{\Delta \varphi}{R_{IF}}. \tag{6}$$

2.2 Description of the model

The studied model represents the cross-section of a 3-wythe brick masonry wall, with a total width of 310 mm. The bricks have dimensions of 200 mm x 95 mm x 50 mm, and the lime-based mortar joints are 15 mm thick. **Figure 2** illustrates the geometry of the cross-section.

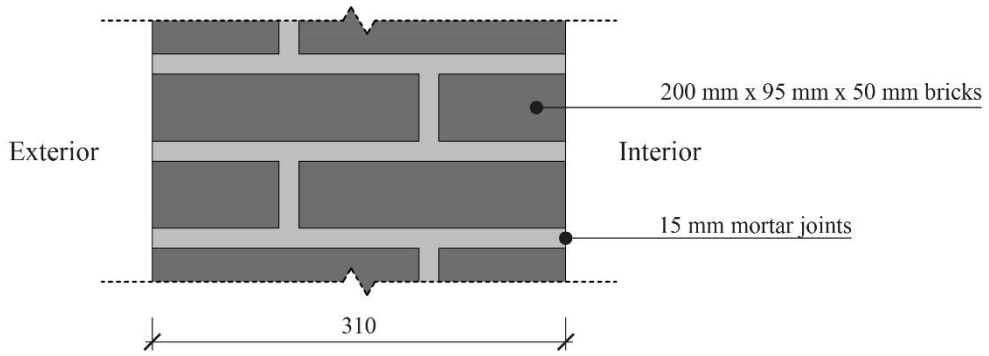

Figure 2. Geometry of the studied wall (dimensions in mm).

The materials properties of brick and mortar employed for the simulations are presented in **Table 1**. Additionally, the interfaces were characterized with a hydraulic resistance value $R_{IF} = 2.0\text{E+9}$ m/s. These properties were collected from relevant studies in the literature [11–14]. It is noted that the sorption isotherm for brick is defined by the following expression:

$$w(\varphi) = w_{cap} \cdot \frac{(\psi - 1)\,\varphi}{\psi - \varphi} \tag{7}$$

On the other hand, the expression proposed by Mualem [15] is used for the equilibrium moisture content curve of the mortar:

$$w(p_c) = w_{cap} \cdot \left[1 + (a \cdot p_c)^{1/(1-m)}\right]^{-m} \tag{8}$$

Table 1. Material properties used in the models.

Property	Symbol	Unit	Brick	Lime mortar
Bulk density	ρ	kg/m^3	1900	2060
Open porosity	ϕ_o	–	0.28	0.23
Capillary moisture content	w_{cap}	kg/m^3	240	190
Fitting parameter for sorption isotherm	ψ	–	1.0070	–
Fitting parameter for adsorption isotherm	a	1/Pa	–	3.8E-6
Fitting parameter for adsorption isotherm	m	–	–	0.352
Water absorption coefficient	A_w	kg/(m^2·s$^{0.5}$)	0.075	0.080
Water vapour resistance factor	μ	–	34.14	15.00
Specific heat capacity	C_p	J/(kg·K)	825	840
Thermal conductivity	λ	W/(m·K)	0.59	0.85

2.3 Initial and boundary conditions

The initial conditions were set to $\vartheta_0 = 20$ °C and $\varphi_0 = 0.5$. Symmetry was applied to the upper and lower boundaries of the wall segment under study. For the thermal analysis, an external temperature of $\vartheta_{ext} = 60$ °C was imposed on the outer surface of the wall, whereas a zero-flux condition, $q_0 = 0$ W/m^2, was applied to the inner surface. Similarly, for the moisture analysis, a relative humidity of $\varphi_{ext} = 1.0$ was imposed on the exterior surface, with a zero-flux condition, $g_0 = 0$ kg/(m^2·s), on the inner face. It is important to note that these boundary conditions do not represent a real-case scenario, but they were selected to facilitate a clearer analysis of heat and moisture transport in building materials.

For the sake of simplicity, isohygral conditions were assumed to study heat transport, with the external and internal relative humidities kept constant and equal to the initial value, $\varphi_{ext} = \varphi_{int} = \varphi_0 = 0.5$. Conversely, for the moisture transport analysis, isothermal conditions were assumed, $\vartheta_{ext} = \vartheta_{int} = \vartheta_0 = 20$ °C.

2.4 Homogenization approaches

The heat and moisture transport analyses were conducted by applying a series of calibration measures according to the type of modelling approach. An averaging procedure was utilized for the discrete micro- and macro-modelling approaches. This procedure involves calculating equivalent properties based on the volume fraction of each material relative to the total volume in the original configuration. The equivalent property X_{EQ} is determined as follows:

$$X_{EQ} = \sum_i^n \left(X_i \frac{V_i}{V_{Total}} \right) \tag{9}$$

Consequently, the equivalent properties for these modelling strategies were calculated based on the parameters presented in **Table 1**, considering a volume fraction of 0.73 for brick and the respective volume fraction of mortar equal to 0.27.

Subsequently, some calibration parameters were employed to analyse the same scenarios considering the continuous micro-, discrete micro-, and macro-modelling approaches. The calibration parameters used in the present study were calculated and validated in a previous work concerning moisture transport on multi-layered masonry specimens [16]. It must be noted that the previous case consisted of water absorption perpendicular to the bed joints, and as it will be shown later, further adjustments would be required to adapt the simulations to transport parallel to the bed joints and thus incorporate the intrinsic orthotropic nature of brick masonry.

For the continuous micro-modelling approach, the brick and mortar were modelled using their original properties. To account for the interfacial impact on moisture flux, the diffusivity factor γ associated with the mortar joints was adjusted accordingly to $\gamma^* = 0.61$.

In the discrete micro-modelling approach, masonry was represented by a combination of two components: bricks were modelled as a continuum with equivalent material properties and extended size, while interfaces were included to simulate mortar joints and brick-mortar boundaries. The primary calibration parameter in this approach was the hydraulic resistance R_{IF} applied at the interfaces, which was updated to ${R_{IF}}^* = 6.0$E+9 m/s.

The macro-modelling approach idealized the masonry as a continuum with homogenized material properties. Similar to the discrete micro-modelling approach, the continuum homogenized material was given equivalent properties calculated using the volume fraction of

each original material. Then, the diffusivity factor γ was used as the calibration parameter, with an updated value of $\gamma^* = 3.08$.

3 RESULTS AND DISCUSSION

The thermal analyses are presented and discussed first. As mentioned above, perfect contact was assumed between the bricks and mortar, thereby neglecting any interface effects. Consequently, the detailed micro- and continuous micro-modelling approaches provide equivalent results, and the same applies for the discrete micro- and macro-modelling approaches. The results obtained using these different strategies are shown in **Figure 3**, illustrating the evolution of temperature over time.

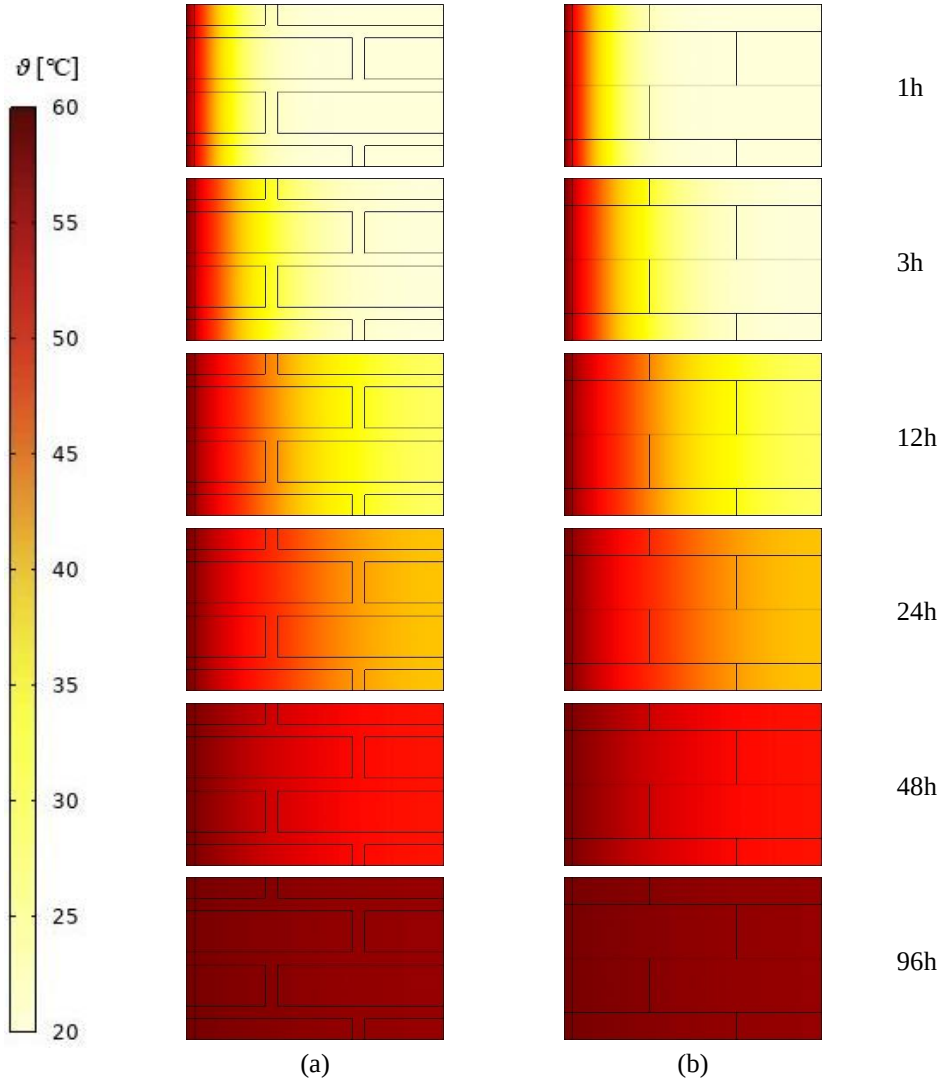

Figure 3. Evolution of temperature in the cross-section of the wall according to different modelling strategies: (a) Detailed micro- and continuous micro-modelling; (b) Discrete micro- and macro-modelling.

The temperature maps reveal a rather homogeneous distribution, which is expected given

the similar thermal properties of the constituent materials. Additionally, the results obtained from the different approaches are very close, supporting the potential for simplification in the study of heat transport in this type of material.

The thermal analysis results are further illustrated in **Figure 4**, which shows the temperature profile evolution across the thickness of the wall. It is noted that the profiles for the detailed micro- and continuous micro-modelling approaches represent the average of three horizontal lines at different representative sections, namely one line through the middle of each course and a third line through the middle of the bed joint. This approach is considered representative due to the homogeneous temperature distribution. The close agreement between the temperature profiles obtained by the different models supports the validity of the approaches and their applicability to thermal problems in such scenarios.

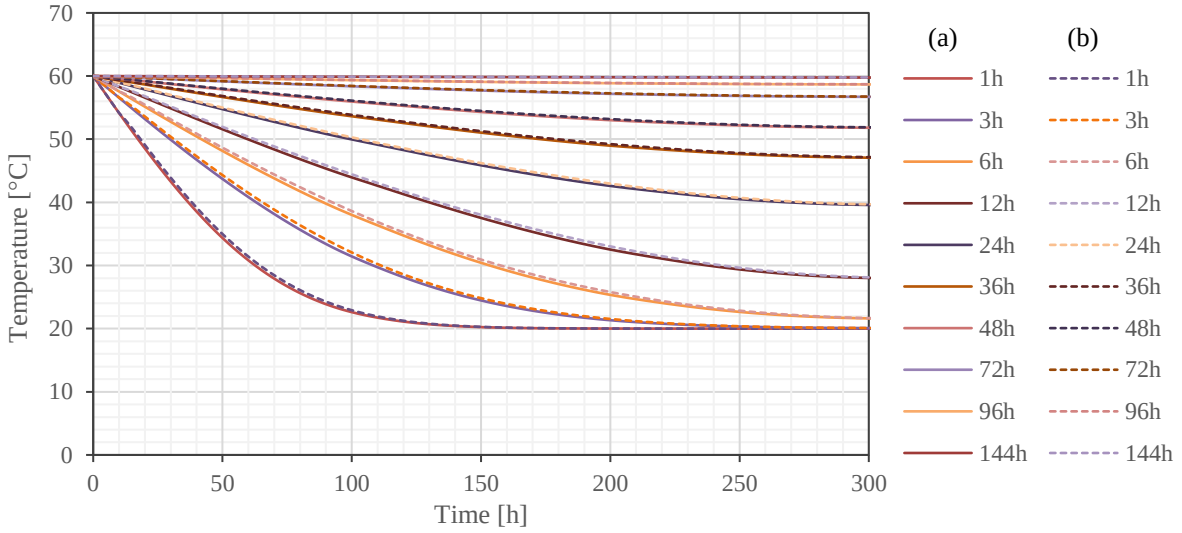

Figure 4. Temperature profiles along the cross-section of the wall according to different modelling strategies: (a) Detailed micro- and continuous micro-modelling; (b) Discrete micro- and macro-modelling.

The moisture transport results obtained from the different modelling strategies are presented in **Figure 5**, which depicts the evolution of internal relative humidity over time. It is shown that the detailed micro-modelling provides the most complex relative humidity distribution. This complexity diminishes as further simplifications are introduced into the model. Additionally, the continuous micro-, discrete micro-, and macro-modelling approaches tend to underestimate the rate of moisture advancement through the cross-section, which is faster according to the detailed micro-modelling results. This discrepancy can be attributed to the calibration strategies used in this study, which were originally validated in moisture absorption tests conducted perpendicular to the bed joints. Consequently, the calibration strategies for those cases aimed to reduce the moisture diffusivity of the mortar and increase the hydraulic resistance of the interfaces in order to reduce moisture flow. However, in the present case, moisture transport is dominated by uninterrupted flow through the bed mortar joint, which, in the case of lime mortar, may even exhibit higher moisture diffusivity than brick. Thus, calibration strategies devised for transport across the bed joints may be less effective here.

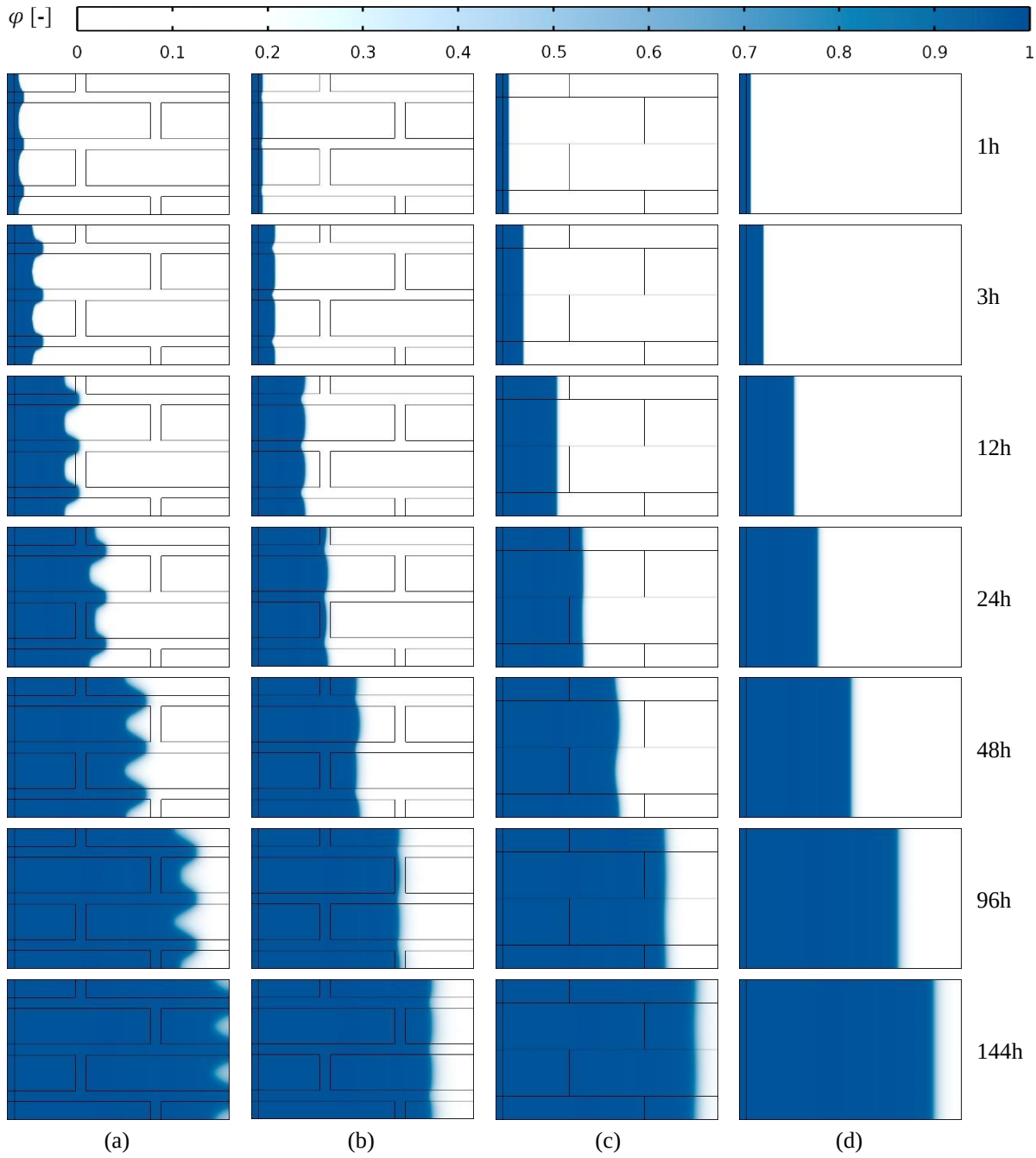

Figure 5. Evolution of relative humidity in the cross-section of the wall according to different modelling strategies: (a) Detailed micro-modelling (for reference); (b) Continuous micro-modelling; (c) Discrete micro-modelling; (d) Macro-modelling.

The moisture transport results are further illustrated in **Figure 6**, which shows the total mass gain in the cross-section area of the wall. The mass gain profiles confirm the visual analysis of relative humidity evolution, highlighting how the implemented simplifications underestimate the speed of moisture ingress into the wall.

For moisture transport, it is clear that the calibration factors derived from experiments

conducted perpendicular to the bed joints cannot be directly applied to cases involving moisture transport parallel to the bed joints. In the former cases, the presence of mortar joints perpendicular to the flow gives rise to interfacial phenomena and the need to artificially reduce the flow through calibration parameters in the simulations. However, for moisture transport parallel to the bed joints, the continuous lime mortar joints serve as preferential paths for moisture ingress, making the previous calibration parameters to reduce the flow ineffective. On the contrary, better results can be obtained when the calibration factors are neglected, and the original properties of the constituent materials (averaged properties for discrete micro- and macro-modelling) and interfaces are used instead (see **Figure 7**). In practice, this means retaining the original values $\gamma = 3.80$ and $R_{IF} = 2.0\text{E+}9$ m/s.

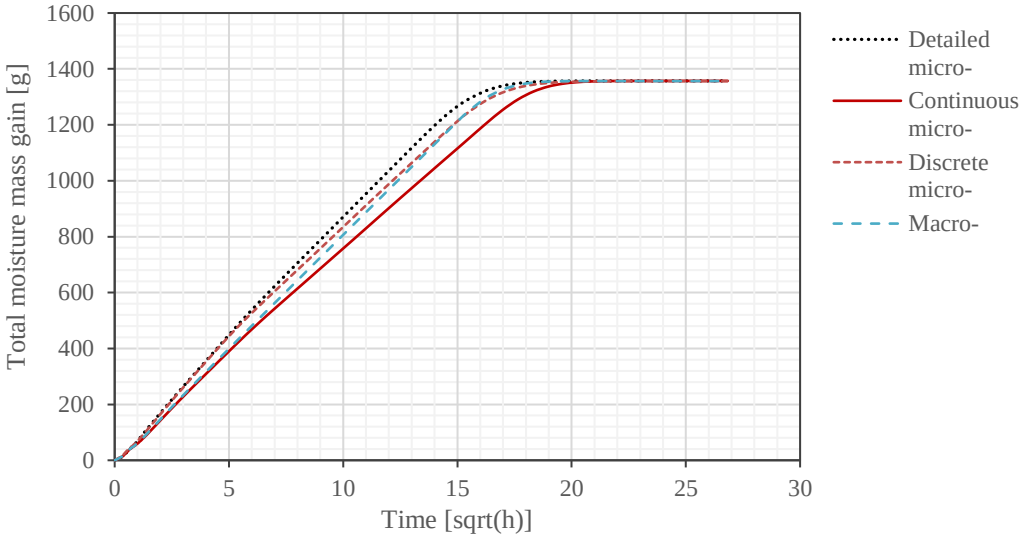

Figure 6. Total mass gain in the cross-section area of the wall according to different modelling strategies.

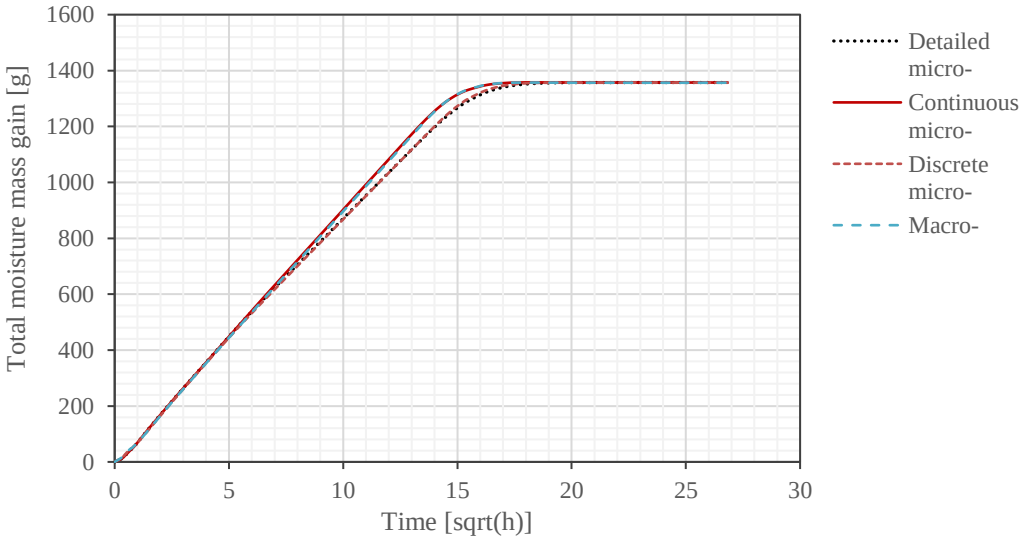

Figure 7. Total mass gain in the cross-section area of the wall neglecting the calibration factors for the different modelling strategies.

4 CONCLUSION

This paper presented the development and application of numerical models to simulate hygrothermal transport in brick masonry. The methodology involved various modelling approaches, including detailed micro-modelling, continuous micro-modelling, discrete micro-modelling, and macro-modelling. Each approach was developed and adjusted based on existing literature to assess the thermal and moisture transport through a representative masonry cross-section subjected to fixed external environmental loads. For simplicity, the heat problem was studied under isohygral conditions, while isothermal conditions were assumed for the study of moisture transport. The models considered perfect interface contact for heat transport and imperfect contact for moisture transport.

The results revealed that thermal transport in masonry can be effectively simulated with simplified models due to the relatively homogeneous distribution of thermal properties across materials. However, moisture transport presented a more complex behaviour, especially in the detailed micro-modelling approach, which highlighted the limitations of simplified models in capturing localized effects. A key limitation identified in this study is the reliance on calibration parameters derived from experiments on water absorption perpendicular to the bed joints, which may not accurately reflect moisture transport parallel to the bed joints. This further underscores the intrinsic orthotropic nature of brick masonry. It is also noted that the conclusions derived from the present study are highly influenced by the choice of materials, namely fired-clay brick and lime-based mortar, both of which have similar thermal and hygric behaviour. Studies on more dissimilar components, such as clay brick and cement mortar, could yield different outcomes. Despite these limitations, the study demonstrates the potential of simplified models to balance computational efficiency and accuracy.

Future research should address the identified limitations through the study of different material combinations, the incorporation of orthotropic properties for bricks, and the evaluation of scenarios under non-isohygral and non-isothermal conditions. Additional experimental validation of moisture transport parallel to bed joints is critical to refine the calibration of the presented models. Moreover, exploring alternative homogenization techniques could enhance the accuracy of macro-modelling approaches, particularly in capturing interfacial phenomena. These advancements would expand the applicability of the models and improve their reliability in predicting the hygrothermal performance of masonry structures.

ACKNOWLEDGMENTS

This work was partly financed by FCT / MCTES through national funds (PIDDAC) under the R&D Unit Institute for Sustainability and Innovation in Structural Engineering (ISISE), under reference UIDB / 04029/2020 (doi.org/10.54499/UIDB/04029/2020), and under the Associate Laboratory Advanced Production and Intelligent Systems ARISE under reference LA/P/0112/2020.

REFERENCES

[1] R. Paolini, A. Zani, M. MeshkinKiya, V.L. Castaldo, A.L. Pisello, F. Antretter, T. Poli, F. Cotana, The hygrothermal performance of residential buildings at urban and rural sites: Sensible and latent energy loads and indoor environmental conditions, Energy Build 152 (2017) 792–803. https://doi.org/10.1016/j.enbuild.2016.11.018.

[2] M. Rahim, R. Djedjig, D. Wu, R. Bennacer, M. EL Ganaoui, Experimental investigation of hygrothermal behavior of wooden-frame house under real climate conditions, Energy and Built Environment 4 (2023) 122–129. https://doi.org/10.1016/j.enbenv.2021.09.002.
[3] A. Blumberga, R. Freimanis, E. Biseniece, A. Kamenders, Hygrothermal Performance Evaluation of Internally Insulated Historic Stone Building in a Cold Climate, Energies (Basel) 16 (2023) 866. https://doi.org/10.3390/en16020866.
[4] B. Ghiassi, P.B. Lourenço, eds., Long-term Performance and Durability of Masonry Structures: Degradation Mechanisms, Health Monitoring and Service Life Design., 1st ed., Woodhead Publishing, Cambridge, UK, 2019. https://doi.org/10.1016/C2016-0-03710-5.
[5] A.M. D'Altri, S. de Miranda, Environmentally-induced loss of performance in FRP strengthening systems bonded to full-scale masonry structures, Constr Build Mater 249 (2020) 118757. https://doi.org/10.1016/j.conbuildmat.2020.118757.
[6] ASTM MNL40, Moisture Analysis and Condensation Control in Building Envelopes, (2001). http://www.astm.org/BOOKSTORE/MNL40PDF/Ch5.pdf.
[7] P.B. Lourenço, Computational strategies for masonry structures, 1996.
[8] M. Petracca, L. Pelà, R. Rossi, S. Zaghi, G. Camata, E. Spacone, Micro–scale continuous and discrete numerical models for nonlinear analysis of masonry shear walls, Constr Build Mater 149 (2017) 296–314. https://doi.org/10.1016/j.conbuildmat.2017.05.130.
[9] A.M. D'Altri, S. de Miranda, G. Castellazzi, V. Sarhosis, A 3D detailed micro–model for the in–plane and out–of–plane numerical analysis of masonry panels, Comput Struct 206 (2018) 18–30. https://doi.org/10.1016/j.compstruc.2018.06.007.
[10] H.M. Künzel, Simultaneous heat and moisture transport in building components: One– and two–dimensional calculation using simple parameters, Ph.D. dissertation, Dept. Building Physics, Fraunhofer Institute for Building Physics, 1995.
[11] R. Ramirez, B. Ghiassi, P. Pineda, P.B. Lourenço, Experimental characterization of moisture transport in brick masonry with natural hydraulic lime mortar, Build Environ 205 (2021) 108256. https://doi.org/10.1016/j.buildenv.2021.108256.
[12] R.D. Prangnell, The water vapour resistivity of building materials: A literature survey, Matériaux et Constructions 4 (1971) 399–405.
[13] V. Kočí, M. Čáchová, D. Koňáková, E. Vejmelková, M. Jerman, M. Keppert, J. Maděra, R. Černý, Heat and Moisture Transport and Storage Parameters of Bricks Affected by the Environment, Int J Thermophys 39 (2018) 63. https://doi.org/10.1007/s10765-018-2383-2.
[14] K. Kumaran, IEA Annex 24: Heat, Air and Moisture Transfer in Insulated Envelope Parts. Final Report, Volume 3, Taks 3: Material Properties, Leuven, Belgium, 1996.
[15] Y. Mualem, A new model for predicting the hydraulic conductivity of unsaturated porous media, Water Resour Res 12 (1976) 593–622.
[16] R. Ramirez, B. Ghiassi, P. Pineda, P.B. Lourenço, Simulation of moisture transport in fired-clay brick masonry structures accounting for interfacial phenomena, Build Environ 228 (2023) 109838. https://doi.org/10.1016/j.buildenv.2022.109838.